JNeurosci
THE JOURNAL OF NEUROSCIENCE

Research Articles: Behavioral/Cognitive

Behavioral and neural dissociation of social anxiety and loneliness

https://doi.org/10.1523/JNEUROSCI.2029-21.2022

Cite as: J. Neurosci 2022; 10.1523/JNEUROSCI.2029-21.2022

Received: 8 October 2021
Revised: 20 January 2022
Accepted: 21 January 2022

Research Article

Behavioral and neural dissociation of social anxiety and loneliness

Jana Lieberz[a,*], Simone G. Shamay-Tsoory[b], Nira Saporta[b], Alisa Kanterman[b], Jessica Gorni[a], Timo Esser[a], Ekaterina Kuskova[a], Johannes Schultz[c,d], René Hurlemann[e,f], Dirk Scheele[a,e,*]

[a] Research Section Medical Psychology, Department of Psychiatry and Psychotherapy, University Hospital Bonn, 53127 Bonn, Germany
[b] Department of Psychology, University of Haifa, Haifa 3498838, Israel
[c] Center for Economics and Neuroscience, University of Bonn, 53127 Bonn, Germany
[d] Institute of Experimental Epileptology and Cognition Research, University of Bonn, 53127 Bonn, Germany
[e] Department of Psychiatry, School of Medicine & Health Sciences, University of Oldenburg, 26129 Oldenburg, Germany
[f] Research Center Neurosensory Science, University of Oldenburg, 26129 Oldenburg, Germany

Abbreviated Title: Dissociation of social anxiety and loneliness

*Corresponding Author:
Jana Lieberz: jana.lieberz@hotmail.de

Dirk Scheele: dirk-scheele@gmx.de

Number of figures: 5, tables: 2
Word count abstract: 250, introduction: 647, discussion: 1563
Keywords: amygdala, fMRI, loneliness, striatum, social anxiety

Conflict of interest statement: The authors declare no competing financial interests.

Acknowledgement: S.G.S-T, R.H., and D.S. are supported by a German-Israel Foundation for Scientific Research and Development grant (GIF, I-1428-105.4/2017). The authors thank Alexandra Goertzen-Patin for proofreading the manuscript and Marie Coenjaerts and Mitjan Morr for helpful discussions about our manuscript.

Abstract

Loneliness is a public health concern with detrimental effects on physical and mental well-being. Given phenotypical overlaps between loneliness and social anxiety (SA), cognitive-behavioral interventions targeting SA might be adopted to reduce loneliness. However, whether SA and loneliness share the same underlying neurocognitive mechanisms is still an elusive question. The current study aimed at investigating to what extent known behavioral and neural correlates of social avoidance in SA are evident in loneliness. We used a pre-stratified approach involving 42 (21 females) participants with high loneliness (HL) and 40 (20 females) participants with low loneliness (LL) scores. During functional magnetic resonance imaging, participants completed a social gambling task to measure the subjective value of engaging in social situations and responses to social feedback. Uni- and multivariate analyses of behavioral and neural data replicated known task effects. However, although HL participants showed increased SA, loneliness was associated with a response pattern clearly distinct from SA. Specifically, contrary to expectations based on SA differences, Bayesian analyses revealed moderate evidence for equal subjective values of engaging in social situations and comparable amygdala responses to social decision-making and striatal responses to positive social feedback in both groups. Moreover, while explorative analyses revealed reduced pleasantness ratings, increased striatal activity, and decreased striatal-hippocampal connectivity in response to negative computer feedback in HL participants, these effects were diminished for negative social feedback. Our findings suggest that unlike SA, loneliness is not associated with withdrawal from social interactions. Thus, established interventions for SA should be adjusted when targeting loneliness.

Significance Statement

Loneliness can cause serious health problems. Adapting well-established cognitive-behavioral therapies targeting social anxiety might be promising to reduce chronic loneliness given a close link between both constructs. However, a better understanding of behavioral and neurobiological factors associated with loneliness is needed to identify which specific mechanisms of social anxiety are shared by lonely individuals. We found that lonely individuals show a consistently distinct pattern of behavioral and neural responsiveness to social decision-making and social feedback compared to previous findings for social anxiety. Our results indicate that loneliness is associated with a biased emotional reactivity to negative events rather than social avoidance. Our findings thus emphasize the distinctiveness of loneliness from social anxiety and the need for adjusted psychotherapeutic protocols.

Introduction

Loneliness is a painful condition with detrimental effects on mental and physical health (Quadt et al., 2020). As such, loneliness has been identified as a risk factor for premature mortality comparable with smoking or obesity (Holt-Lunstad et al., 2010). Consequently, loneliness has come into focus of politics and clinicians as a major public health concern with high economic costs for society (Jeste et al., 2020; Mihalopoulos et al., 2020). With social distancing measures in most countries around the world, COVID-19 is expected to have vast impact on physical and mental health, particularly in people inflicted by poor resilience to social adversity due to pre-existing low levels of social integration (Galea et al., 2020; Vindegaard & Benros, 2020), emphasizing the urgent need of interventions to target loneliness. Adjusting established cognitive-behavioral therapies targeting related psychopathology such as depression or social anxiety (SA) (Heinrich & Gullone, 2006) seems promising to accelerate the development of treatments to reduce loneliness. However, previous studies indicated that loneliness and depression are distinct constructs based on unique neurobiological mechanisms (Cacioppo et al., 2010; Shao et al., 2019). Conversely, it is still unclear whether loneliness shares neurobiological substrates with SA, which would allow rapid co-optations of psychotherapeutic protocols.

Recent findings highlight close links between loneliness and SA symptoms (Bruce et al., 2019; Maes et al., 2019) and identified SA as predictor for future loneliness (Lim et al., 2016; Danneel et al., 2019). For instance, SA was found to be consistently associated with social isolation, lower perceived social support, and poor friendship quality, resulting in decreased relationship satisfaction which is a key feature of loneliness (Peplau & Caldwell, 1978; Teo et al., 2013; Porter & Chambless, 2014; Rapee et al., 2015; Rodebaugh et al., 2015). Likewise, the avoidance of social situations is known to be a core mechanism of SA and although

100 loneliness might have evolved as a motivation to reconnect with others, social avoidance is
101 also hypothesized to be preferred by lonely individuals (Cacioppo & Cacioppo, 2018).

102 Existing SA intervention programs are often based on cognitive models of SA (Clark & Wells,
103 1995), which posit an exaggerated fear of evaluation as a core etiological mechanism of
104 psychopathology. Indeed, current neurocircuitry models of SA disorder emphasize amygdala
105 hyperreactivity to social stimuli (Etkin & Wager, 2007; Bruhl et al., 2014). Conversely, the
106 neural responsiveness to social rewards seems to be reduced in individuals with SA (Richey
107 et al., 2017; Schultz et al., 2019), potentially resulting in reduced positive affect in response
108 to social interactions (Kashdan & Collins, 2010). Similarly, lonely individuals exhibit
109 attenuated responsiveness to positive social interactions (Lieberz et al., 2021) and
110 preliminary evidence indicates that alterations in amygdala structure and function are
111 associated with loneliness (for a comprehensive review of neurobiological correlates of
112 loneliness, see Lam et al. (2021)).

113 The current study therefore aims at examining whether mechanisms underlying SA could
114 also underlie loneliness. We recruited a pre-stratified sample of 42 healthy participants with
115 high (high-lonely, HL) and 40 participants with low (low-lonely, LL) loneliness scores. During
116 functional magnetic resonance imaging (fMRI), the participants completed a social gambling
117 task as used by Schultz et al. (2019) to measure the behavioral and neural responsiveness
118 to social decision-making and social feedback. Given the intertwined phenotype of SA and
119 loneliness, we hypothesized that lonely individuals would show increased SA
120 symptomatology and in turn behavioral and neural response patterns associated with social
121 avoidance (cf. Schultz et al. (2019)). Specifically, we hypothesized decreased subjective
122 values of engaging in social situations, increased amygdala activation during social decision-
123 making and social feedback, and decreased reward-associated responses of the nucleus
124 accumbens (NAcc) to positive social feedback in lonely participants. Moreover, we explored
125 distinct behavioral and neural response patterns in loneliness that have not been previously

found to be associated with SA (i.e., responsiveness to negative social feedback). We controlled for the influence of SA and further potential confounding variables for all observed correlates of loneliness.

Materials and Methods

Participants

We recruited a sample of 82 (out of a stratified sample of 3678 adults; 41 females, mean age ± standard deviation (SD): 26.83 ± 7.47 years, see Lieberz et al. (2021)) pre-stratified healthy HL (n = 42) and LL volunteers (n = 40) as assessed by the revised version of the UCLA loneliness scale (UCLA-L, Russell et al. (1980)). HL Participants were characterized by UCLA-L scores of 50 or above (i.e., at least one standard deviation above the mean score of students, cf. Russell et al. (1980)), while LL participants were characterized by scores of 25 or below (i.e., at least one standard deviation below the mean score of young adults). All participants fulfilled the following inclusion criteria: aged 18-65, no current physical or psychiatric disorder as assessed via self-disclosure and by the Mini-International Neuropsychiatric Interview (Sheehan et al., 1998), no psychotherapy, no current psychotropic medication, no illicit drug use in the previous four weeks, right-handed, eligibility for MRI scanning. The sample size was based on an a-priori power analysis (cf. Lieberz et al. (2021)). The analysis using G*Power 3 (Faul et al., 2007) indicated that at least 71 participants were needed to reliably replicate a previously reported loneliness effect on ventral striatum/amygdala activity (Cacioppo et al., 2009) with a power of 0.99 ($\alpha = 0.05$). To account for possible missing data and drop-outs, we planned to test at least 80 participants, resulting in the final sample size of 82 participants. For a comprehensive description of the pre-stratification approach, see Lieberz et al. (2021).

All participants gave written informed consent. The study was approved by the institutional review board of the Medical Faculty of the University of Bonn (study number 016/18) and conducted in accordance with the latest revision of the Declaration of Helsinki.

154

155 **Experimental design and statistical analyses**

156 Following the screening of inclusion criteria, participants completed a virtual auction task to
157 measure the individual monetary value associated with receiving positive or avoiding
158 negative social feedback. To further measure the participants' subjective value of engaging
159 in social situations, participants competed a social gambling task (cf. Schultz et al. (2019))
160 during a separate test session and repeated the task during fMRI on the same day. Data
161 collection was completed before the start of the COVID-19 pandemic. The analysis plan was
162 preregistered prior to conducting any analyses (https://osf.io/x47ke). All data used in this
163 study are openly available (https://osf.io/p6jxk/ and
164 https://neurovault.org/collections/VNYRMORR/).

165

166 **Social gambling task**

167 Each trial of the social gambling task consisted of a decision and a feedback stage (see **Fig.**
168 **1**). During the decision phase, participants could choose a risky (a dice game with a virtual
169 human or computer partner with equiprobable outcomes of 3 or 0 €) or a safe option (a fixed
170 payoff ranging from 0 to 3 € in steps of 50 cents) with no imposed time limit. Human partners
171 were indicated by the name and picture of one out of four partners while the computer control
172 condition was indicated by a picture of a computer. If participants chose the risky option,
173 either a positive or a negative feedback video of the partner (human or computer) was shown
174 (feedback phase), depending on the outcome of the trial (win or loss). As such, the human
175 feedback video displayed the virtual human partner expressing either admiration or
176 condescension. All human pictures and videos were taken from a validated database
177 (Kaulard et al., 2012). In the computer control condition, the feedback was given by a video
178 of a checkmark (participant won) or a cross (participant lost). Each feedback video was

presented two times in immediate succession. If participants chose the safe option, a sentence confirmed the payoff. Each human partner was paired twice with each possible amount of money offered as alternative for the risky option, resulting in 56 trials. Likewise, participants completed 56 trials of the control condition. After finishing the task, participants rated the pleasantness of each positive and negative feedback video on a visual analogue scale ranging from 0 (“not pleasant at all”) to 100 (“very pleasant”). Moreover, for each participant, individual certainty equivalents of the risky option (termed CE50), i.e., the certain payoff for which a participant would be indifferent between the risky and safe options (i.e., they would choose each option with equal probability), were estimated separately for the computer and the human partners by fitting participants’ choices as a function of the difference between the expected values of the safe and risky options with a cumulative Gaussian function. CE20 and CE80, i.e., certain payoffs associated with choosing the safe option with respectively 20 % and 80 % probability, were similarly estimated. The subjective value of engaging in social situations was defined as the individual difference between the estimated CE50 for human partners compared to the computer partner.

The task was repeated during fMRI with the following adjustments: the partner for each trial (one of four human partners or the computer) was chosen randomly and indicated by the name of the partner (no face was shown at this stage) or the word “computer”. Furthermore, the fixed payoff offered in the safe option varied randomly between the three individually determined values CE20, CE50, and CE80. Using individualized payoffs as a safe alternative enabled us to equate the number of risky and safe choices across participants. Participants responded with their index fingers using an MRI-compatible response grip system (NordicNeuroLab AS, Bergen, Norway). The position of the risky option (left or right on the screen) was counterbalanced across trials. All human partners were presented in combination with each of the three CE values twice, resulting in 24 human trials and 24 computer trials per run. The feedback video was presented two times during a fixed time interval of 2.6 seconds. The temporal intervals between the decision and outcome stages

and the inter-stimulus intervals between trials varied from 2 to 11 seconds with a descending probability. All participants completed two runs. Participants received the obtained money from one randomly chosen trial per run. To summarize, this task allowed us to obtain an experimental measure of social avoidance behavior (specifically, the difference in subjective values between engaging in an interaction with a person or a computer) and its associated neural signal (amygdala hyperactivity during social decision-making, amygdala hypersensitivity to human feedback, and reduced reward-associated brain activity in response to positive human feedback). Thus, the task enabled us to concurrently explore behavioral and neural response patterns associated with social avoidance and social feedback processing as core mechanisms underlying the persistence of SA.

Virtual auction task

We further measured the individual monetary value associated with receiving positive or avoiding negative social feedback during a virtual auction task. Specifically, participants were informed that they were participating in a virtual auction against the computer using a random algorithm to invest money. In each trial, a picture of one of six actors indicated which feedback video was being auctioned. The same actors and videos as included in the social gambling task were used plus two additional actors from the same database (see above). In each trial, participants were asked with no imposed time limit to invest any amount of money between 0 € and 1 € at their disposal (in increments of 5 cents) to (1) increase the probability of watching a positive social feedback video or (2) to decrease the probability of watching a negative social feedback video. There were six trials in the positive and six trials in the negative feedback conditions. After completion of all trials, one trial was chosen randomly and the invested money was compared to a randomly selected amount representing the money invested by the computer. The player (participant or computer) who invested more money won the auction, received the outcome of the trial and kept the remaining money (1 €

minus the invested money). As the investments of the computer were based on uniformly distributed random investments between 0 € and 1 €, each cent invested by the participant corresponded to a probability change of 1% to win the auction. In the positive feedback condition, a positive social feedback video (expressing admiration) was presented if the participant won the auction, while no video was presented if the participant lost. In the negative feedback condition, a negative social feedback video (expressing condescension) was presented if the participant lost and no video was shown if the participant won. If the participants lost, they kept 1 €, irrespective of the invested money. The feedback videos were repeated until the participants pressed any key. Notably, winning the auction was associated with a smaller monetary payout than losing the auction. This way, the virtual auction task enabled us to explore whether receiving positive social feedback or avoiding negative feedback would be worth a higher monetary loss for HL compared to LL participants.

fMRI data acquisition and preprocessing

All fMRI data were acquired using a 3T Siemens TRIO MRI system (Siemens AG, Erlangen, Germany) with a Siemens 32-channel head coil. Functional data of the social gambling task were acquired using a T2*-weighted echoplanar (EPI) sequence with a repetition time (TR) of 2500 ms, an echo time (TE) of 30 ms, ascending slicing, a matrix size of 96 x 96, 37 axial slices with a voxel size of 2 x 2 x 3 mm^3 and a slice thickness of 3.0 mm, a distance factor of 10 %, a field of view (FoV) of 192 x 192 mm^2, and a flip angle of 90°. High-resolution T1-weighted structural images were collected on the same scanner (TR = 1660 ms, TE = 2.54 ms, matrix size: 256 x 256, voxel size: 0.8 x 0.8 x 0.8 mm^3, slice thickness = 0.8 mm, FoV = 256 x 256 mm^2, flip angle = 9°, 208 sagittal slices). To control for inhomogeneity of the magnetic field, fieldmaps were obtained for the T2*-weighted EPI sequence (TR = 392 ms, TE [1] = 4.92, TE [2] = 7.38, matrix size: 64 x 64, voxel size: 3 x 3 x 3, slice thickness = 3.0 mm, distance factor = 10 %, FoV = 192 x 192 mm^2, flip angle 60°, 37 axial slices). For

preprocessing, standard procedures of SPM12 (Wellcome Trust Center for Neuroimaging, London, UK; https://www.fil.ion.ucl.ac.uk/spm/) implemented in Matlab (The MathWorks Inc., Natick, MA) were used. The first five volumes of each functional time series were removed to allow for T1 signal equilibration before affine registration was used to correct for head movements between scans. Images were initially realigned to the first image of the time series and then re-realigned to the mean of all images. For unwarping, the voxel displacement map (VDM file) was applied to the EPI time series to correct for signal distortion based on B0-field inhomogeneity. Normalization parameters as determined by segmentation and non-linear warping of the structural scan to reference tissue probability maps in Montreal Neurological Institute (MNI) space were applied to all functional images. All images were resampled at 2 x 2 x 2 mm^3 voxel space and spatially smoothed by using a 6-mm full width half maximum (FWHM) Gaussian kernel. A high-pass filter with a cut-off period of 128 s was used to detrend raw time series.

Behavioral data analysis

Behavioral data were analyzed in SPSS 24 (IBM Corp., Armonk, NY). Specifically, to analyze the social gambling task, we calculated mixed-design analyses of variance (ANOVAs) with the estimated CE50 values, the proportion of safe decisions during the behavioral and the fMRI task, and the pleasantness ratings of the feedback videos as dependent variables. For all analyses, group (HL vs. LL) served as between-subject factor and the partner condition (human vs. computer) was included as within-subject factor. Offered payoffs as safe option were further included as within-subject factor for the behavioral task (0 € to 3 € in steps of 50 cents) and the fMRI task (CE20, CE50, CE80) to analyze the proportion of safe decisions, whereas the analysis of the pleasantness ratings of the feedback videos included the additional within-subject factor feedback valence (positive vs. negative feedback). For task validation, we first tested whether differences between participant groups replicated the SA

284 effects reported by Schultz et al. (2019). Thus, we examined whether increasing safe option
285 payoffs were associated with increased proportions of safe decisions in both behavior and
286 fMRI tasks (main effect of payoff), and whether positive feedback was rated as more
287 pleasant compared to negative feedback (main effect of feedback valence). Moreover, we
288 tested whether we could replicate the previously observed negative association between SA
289 (measured by the Liebowitz Social Anxiety Scale, LSAS (Liebowitz, 1987)) and social
290 engagement in participants unaffected by loneliness, i.e., the LL group. We then examined
291 the hypothesized effects of loneliness on the subjective value of engaging in social situations
292 and explored loneliness effects on the pleasantness ratings of the feedback videos.

293 For the analysis of the virtual auction task, effects of the valence (positive vs. negative video)
294 and group were included as within- and between-subject factors, respectively, in a mixed-
295 design ANOVA with invested money serving as dependent variable. Greenhouse-Geisser
296 corrections were applied in cases of violated assumptions of sphericity as tested by
297 Mauchly's test. All post-hoc t-tests to disentangle interactions were Bonferroni-corrected
298 (P_{cor}). *P*-values < 0.05 (two-tailed) were considered significant.

299

300 **fMRI data analysis**

301 To analyze the fMRI data, we used a two-stage approach as implemented in SPM12. On the
302 first level, data were modeled using a fixed-effects model. Onsets and durations of eight
303 conditions ('risky decision computer', 'safe decision computer', 'risky decision human', 'safe
304 decision human', 'positive computer feedback, 'negative computer feedback', 'positive
305 human feedback', 'negative human feedback') were modeled by a stick function convolved
306 with a hemodynamic response function (HRF). Although individual CE values were used
307 during the fMRI task to equalize the number of trials of each condition between both runs, the
308 decisions of the participants and thereby the resulting number of trials of one condition still

differed between runs to varying degrees. We thus decided to concatenate time series of both runs (cf. Cho et al. (2020)). Baseline regressors were added for each run, and the high-pass filter and temporal non-sphericity estimates were adjusted separately for each run. The six movement parameters were included in the design matrix as regressors of no interest. Within-subject contrasts of interest were calculated on the first level and entered to a random-effects model on the second level. For task validation, one-sample t-tests were calculated across groups (i.e., decision human > decision computer, risky decision human > risky decision computer, safe decision human > safe decision computer, human feedback > computer feedback, positive feedback > negative feedback). Furthermore, whole-brain task effects (e.g., decision human > decision computer) were analyzed across groups after applying an initial cluster-forming height threshold of $P < 0.001$. Additional whole-brain analyses were calculated to examine neural responses during decision-making (risky decision vs. safe decision) and feedback processing (positive vs. negative human feedback) in the social gambling task. To further validate whether the previously observed association between SA and increased amygdala activation during social decision-making (risky decision human > safe decision human and risky decision human > risky decision computer) and while receiving human feedback (human feedback > computer feedback) could be replicated in our sample, we extracted parameter estimates of the anatomically-defined amygdala for these contrasts and correlated the averaged activity across voxels with SA scores. Likewise, we analyzed the association between SA and increased NAcc response to positive human compared to positive computer feedback. To ensure that a replication of SA-related findings was not driven by loneliness, we included only participants of the LL group in this analysis.

We then assessed group-specific response patterns by calculating two-sample t-tests. Specifically, to probe the hypothesis of increased amygdala activation during social decision-making in HL participants, we compared brain activity during risky decisions involving a human partner between groups (i.e., $HL_{\text{risky decision human > safe decision human}} > LL_{\text{risky decision human > safe decision human}}$, $HL_{\text{risky decision human > risky decision computer}} > LL_{\text{risky decision human > risky decision computer}}$). Likewise,

the hypothesized increased amygdala responsiveness to human feedback ($HL_{\text{human feedback > computer feedback}} > LL_{\text{human feedback > computer feedback}}$) and reduced NAcc reactivity to positive human feedback ($LL_{\text{positive human feedback > positive computer feedback}} > HL_{\text{positive human feedback > positive computer feedback}}$) were tested. As the behavioral data indicated an altered responsiveness to negative human feedback (see behavioral results), we explored group differences in response to negative human feedback ($HL_{\text{negative human feedback > negative computer feedback}} > LL_{\text{negative human feedback > negative computer feedback}}$). These contrasts were also calculated in the opposite direction (e.g., $LL_{\text{risky decision human > risky decision computer}} > HL_{\text{risky decision human > risky decision computer}}$). The amygdala and NAcc were anatomically defined according to the Wake Forest University PickAtlas (Maldjian et al., 2003; Maldjian et al., 2004). *P*-values < 0.05 after familywise error correction for multiple testing (P_{FWE}) based on the size of the respective region of interest were considered significant. Additional explorative whole-brain analyses were calculated to compare brain activation between groups for the contrasts of interest. Parameter estimates of clusters showing significant group effects were extracted and further analyzed in SPSS 24 to disentangle the group x task condition interaction. Behavioral group effects were correlated with parameter estimates of neural group effects by calculating Pearson's product-moment correlations. Five participants were excluded from fMRI analyses due to excessive head movement (> 4 mm/° in any direction; *n* = 2), anatomical abnormalities (*n* = 1), technical issues (*n* = 1), or incomplete data (*n* = 1). Furthermore, three participants were excluded from analyses of the decision stage as they always chose the risky option for at least one of the partners, while one participant was excluded from analyses of the feedback stage because no positive human feedback was shown during both runs.

Multivariate pattern analysis

We conducted a multivariate pattern analysis using the Decoding Toolbox (Hebart et al., 2014) as further task validation and to probe the replicability of the previous finding that

362 decisions of the participants could be decoded from amygdala activation (cf. Schultz et al.
363 (2019)). Notably, rather than re-analyzing the involvement of the amygdala in social decision-
364 making as examined by the univariate task validation, the multivariate pattern analysis was
365 used to verify the involvement of the amygdala in decision-making processes irrespective of
366 the specific partner (human or computer). For the decoding analysis, we used non-
367 normalized and unsmoothed data of each participant and included the same conditions and
368 regressors as outlined above in the single-subject fixed-effects models separately for both
369 runs. The participants' decisions (risky or safe decision) were used as independent variables
370 and parameter estimates of the corresponding first level regressors were used as features.
371 Using the default parameters of the Decoding Toolbox, we ran a classification searchlight
372 analysis with a 9-mm searchlight radius and trained a support vector machine classifier
373 (LIBSVM) on the data of one run to decode the decision to play or to choose the safe option.
374 The decoding accuracy was tested on the data of the other run and the resulting individual
375 accuracy maps minus chance (chance = 50 % accuracy) were normalized to MNI space and
376 smoothed using a 6-mm FWHM Gaussian kernel. Maps of accuracy minus chance decoding
377 performance were then entered into a random-effect model on the second level and tested
378 against 0 by calculating a one-sample t-test across groups. Familywise error (FWE)
379 correction was applied based on the size of the anatomically defined amygdala (cf. Schultz et
380 al. (2019)). Furthermore, we explored whether the amygdala activation-based decision
381 decoding accuracy during general decision-making (i.e., across human and computer
382 partners) differed between groups by calculating a two-sample t-test.

383

384 **Functional connectivity analyses**

385 Given that social decision-making and the processing of social rewards rely on complex
386 neural networks rather than on single brain regions (Ruff & Fehr, 2014) and given previously
387 reported associations between SA and altered functional connectivity between the involved

388 brain regions (i.e., amygdala or NAcc) and other brain regions (Schultz et al., 2019), we
389 searched for loneliness-related changes in functional connectivity with the same seed
390 regions (amygdala or NAcc) and other brain regions. Contrasts revealing significant group
391 effects in the univariate activity analyses (see above) were thus examined by exploratory
392 generalized psychophysiological interaction (gPPI) analyses using the CONN toolbox 19.b
393 (www.nitrc.org/projects/conn, RRID:SCR_009550). Following the recommendations of the
394 CONN toolbox, preprocessing for the gPPI analyses additionally included a denoising
395 pipeline. Outlier scans were detected by the integrated artefact detection toolbox-based
396 identification using conservative settings (i.e., thresholds of 0.5 mm frame wise displacement
397 and 3 SD above global BOLD signal changes were used) and treated as regressors of no
398 interest in the following analyses. The default denoising pipeline implemented a linear
399 regression of confounding effects of the first five principal noise components from white
400 matter and cerebrospinal fluid template masks, 12 motion parameters, scrubbing, and
401 constant task-related effects. A high-pass filter of 0.008 Hz was applied to minimize the
402 effects of physiological and motion related noise. Regions associated with group effects
403 (amygdala or NAcc) served as seed regions in a seed-to-voxel analysis. The interaction
404 terms of the psychological (task conditions convolved with a canonical HRF) and the
405 physiological factor (blood oxygenation level dependent signal) were computed for each
406 participant on the first level. The relative measure of connectivity compared to the implicit
407 baseline was calculated by using bivariate regression measures. Connectivity was compared
408 between groups on the second level by using mixed-design ANOVAs.

409

410 **Bayesian analyses**

411 The main purpose of the current study was to investigate whether HL participants differ from
412 LL participants in variables associated with core etiological mechanisms of SA. While
413 frequentist analyses allow to interpret the significance of an observed group difference, a

non-significant result cannot be interpreted as evidence for the equivalence of groups (Keysers et al., 2020). However, evidence for comparable neural responses to social stimuli and during social decision-making in HL and LL participants would have important clinical implications as this would indicate that loneliness is not associated with neurobiological mechanisms of SA which are the targets of cognitive-behavioral therapy manuals. Importantly, Bayesian analyses are able to distinguish between the absence of evidence (i.e., more data are needed to interpret the results) and evidence for the absence of an effect and are thus recommended to complement frequentist analyses (Keysers et al., 2020). Therefore, for all hypothesized differences between HL and LL participants that could not be confirmed by classical inference analyses, Bayesian t-tests were conducted to quantify the evidence for the null hypotheses (i.e., HL participants do not differ from LL participants) using the default settings for two-tailed independent t-tests implemented in JASP (JASP Team, 2020). Specifically, group differences in the subjective value of engaging in social situations during the social gambling task (i.e., the individual CE50 for human partners minus CE50 for the computer partner) and pleasantness ratings of positive human feedback (minus the ratings of positive computer feedback) were re-analyzed by calculating Bayesian t-tests. Moreover, as we expected HL participants to differ from LL participants regarding amygdala responsiveness to risky decisions involving a human partner, parameter estimates of the anatomically-defined amygdala response during the decision stage were averaged across all voxels and re-analyzed to quantify evidence of differences between groups for the following contrasts of interest: risky decision human > risky decision computer and risky decision human > safe decision human. Likewise, parameter estimates of activation during the feedback stage were extracted from the amygdala to re-analyze responsiveness to human feedback (compared to computer feedback). To re-analyze reward-associated brain activity in response to positive human feedback (compared to computer feedback), parameter estimates were extracted from the NAcc.

441 **Mediation and moderation analyses**

442 For variables that were found to be associated with SA in the LL group, we calculated
443 moderation analyses to investigate whether group (HL vs. LL) moderated the size of SA
444 effects. A significant interaction between group and SA would thus indicate that the
445 association between SA and the dependent variable would differ between HL and LL
446 participants. Moderation analyses were calculated for amygdala activation during social
447 decision-making (risky decision human > safe decision human and risky decision human >
448 risky decision computer) and for the subjective values of engaging in social situations as
449 dependent variables, SA scores as independent variable, and group as moderator. Again,
450 parameter estimates were averaged across all voxels of the anatomical amygdala.

451 Likewise, we conducted moderation analyses to examine whether the differences in negative
452 feedback processing between HL and LL participants differed as a function of SA (i.e.,
453 whether the associations between loneliness and the dependent variables were weakened or
454 enhanced for participants with high SA scores). Thus, group (HL or LL) was used as
455 independent variable to analyze those dependent variables that showed differences between
456 groups, and SA was included as moderator variable. In addition to the investigation of
457 interaction effects between group and SA, we examined whether the observed differences
458 between HL and LL participants could be explained by increased SA in HL participants.
459 Therefore, mediation analyses were calculated with group serving as independent variable
460 and SA serving as mediator.

461 To examine the influence of further possible confounding variables on significant group
462 effects (i.e., depressive symptomatology assessed by the Beck's Depression Inventory II,
463 BDI (Beck et al., 1996) and childhood maltreatment assessed by the Childhood Trauma
464 Questionnaire, CTQ (Bernstein et al., 1994)), we calculated mediation and moderation
465 analyses using the PROCESS macro v3.4 for SPSS (Hayes, 2017). BDI and CTQ scores
466 were used as mediator and moderator variables and group as predictor variable. Again,

467 mediation analyses were calculated to examine whether observed differences between
468 groups might be driven by differences in psychiatric symptomatology, whereas moderation
469 analyses were conducted to investigate a potential interaction of loneliness (HL vs. LL) with
470 the moderation variable. For mediation analyses, 10,000 bootstrap samples were used.
471 Variables were mean-centered before calculating moderation analyses. Mediations were
472 considered significant if the 95 % confidence interval (CI) of an indirect effect excluded zero
473 while moderations were considered significant if $P < 0.05$ for the interaction effect of group
474 with the potential moderator. Moreover, we further examined whether the observed effects of
475 group remained significant ($P < 0.05$ for the direct effect of group) after including the potential
476 confounding variables (SA, BDI, and CTQ scores) as covariates in the regression model to
477 probe the robustness of the observed explorative loneliness-related findings.

Results

Behavioral results

As expected, SA was significantly increased in HL participants ($t(67.74) = 3.25$, $P = 0.002$, $d = 0.72$; mean LSAS score ± SD in HL: 18.64 ± 15.91, range: 0 to 86; LL: 9.28 ± 9.56, range: 0 to 48; see Lieberz et al. (2021) and **Fig. 2A**) and task effects of the social gambling task reported by Schultz et al. (2019) were replicated across groups: the proportion of safe decisions in the behavioral social gambling task significantly increased with higher payoffs offered as safe alternative to the risky gambling decision across groups (main effect of offered payoff: $F(2.95,236.14) = 183.77$, $P < 0.001$, $\eta_p^2 = 0.70$; see **Fig. 2B**) and was highest for an offered payoff of 3 € (mean proportion of safe decisions ± SD for an offered payoff of 0 €: 8.16 ± 17.06 %; 0.5 €: 8.38 ± 16.44 %; 1 €: 19.36 ± 28.44 %; 1.5 €: 37.96 ± 36.12 %; 2 €: 76.98 ± 30.70 %; 2.5 €: 84.98 ± 25.85 %; 3€: 88.11 ± 23.48 %). Likewise, the proportion of safe decisions differed between all three payoffs offered during the fMRI implementation of the task (main effect of offered payoff: $F(2,158) = 185.43$, $P < 0.001$, $\eta_p^2 = 0.70$; post-hoc comparisons: CE20 vs. CE50: $t(80) = 8.27$, $P_{cor} < 0.001$, $d = 1.08$; CE50 vs. CE80: $t(80) = 11.02$, $P_{cor} < 0.001$, $d = 1.44$; mean proportion of safe decisions ± SD for an offered payoff of CE20: 12.13 ± 18.91 %; CE50: 41.57 ± 32.27 %; CE80: 82.30 ± 22.69 %). Importantly, as individual payoffs were calculated for the fMRI task separately for human and computer partners to equalize the ratio of risky and safe decisions, the likelihood of safe decisions during fMRI differed neither between partners nor between groups (HL vs. LL) (all main effects or interactions of the partner condition or group Fs < 1.48, Ps > 0.05). As intended, positive feedback videos were rated as more pleasant than negative ones (main effect of feedback valence: $F(1,80) = 174.73$, $P < 0.001$, $\eta_p^2 = 0.69$). SA was indeed negatively associated with the subjective value of engaging in social situations in the LL group, but the correlation failed to reach significance ($r(38) = -0.22$, $P = 0.21$).

However, contrary to previously observed effects of SA (Schultz et al., 2019), loneliness (HL vs. LL) affected neither the subjective value of engaging in social situations during the behavioral social gambling task nor investments in the virtual auction task (all *P*s > 0.05). Nevertheless, analyses of pleasantness ratings of the feedback videos revealed a significant interaction of group x partner x feedback valence ($F(1,80) = 4.02$, $P = 0.048$, $\eta_p^2 = 0.05$). To disentangle the interaction, we calculated further mixed-design ANOVAs separately for the positive and negative feedback videos. Surprisingly, no group effects were observed for positive feedback (all *P*s > 0.05), but we found a significant interaction of group x partner for negative feedback ($F(1,80) = 4.34$, $P = 0.04$, $\eta_p^2 = 0.05$; see **Fig. 2C**): HL participants rated the negative human feedback as more pleasant compared to the negative computer feedback ($t(41) = 2.09$, $P_{cor} = 0.09$), while LL participants showed the opposite pattern of ratings ($t(39) = -0.82$, $P_{cor} = 0.84$). Two additional explorative post-hoc tests indicated that HL participants rated the negative computer feedback as less pleasant compared to LL participants (HL vs. LL: $t(80) = -2.09$, $P_{cor} = 0.08$; mean pleasantness ratings ± SD in HL participants: 25.91 ± 22.94; LL: 36.85 ± 24.38), whereas group differences vanished when negative feedback was provided by a human partner ($t(80) = 0.34$, $P_{cor} \approx 1.00$; mean pleasantness ratings± SD in HL participants: 34.77 ± 15.28; LL: 33.68 ± 14.29).

fMRI results

Multi- and univariate analyses of neural activation across groups replicated all previous task effects (Schultz et al., 2019). As such, a linear support vector machine classifier based on amygdala activation was able to decode the decision (risky vs. safe) significantly better than chance (mean accuracy ± SD = 53.64 ± 9.07 %; 30, -4, ,28, $t(73) = 3.45$, $P_{FWE} = 0.048$). Amygdala activation increased during decisions involving a human partner compared to the computer partner (right: 22, -6, -12, $t(73) = 3.68$, $P_{FWE} = 0.03$; left: -22, -8, -12, $t(73) = 4.00$, $P_{FWE} = 0.01$). Specifically, amygdala activity was enhanced during trials in which participants

chose the risky option with a human partner compared to the computer partner (right: 22, -6, -12, $t(73) = 4.58$, $P_{FWE} = 0.002$; left: -22, -8, -12, $t(73) = 4.23$, $P_{FWE} = 0.006$; see **Fig. 3A**), while no differences in amygdala activity between partners were observed for safe decisions. Moreover, receiving feedback from the human partner activated the amygdala significantly stronger than computer feedback (right: 22, -6, -14, $t(75) = 9.67$, $P_{FWE} < 0.001$, left: -22, -8, -12, $t(75) = 9.66$, $P_{FWE} < 0.001$) and NAcc activity was increased in response to positive feedback compared to negative feedback across partner types (right: 12, 8, -6, $t(75) = 6.45$, $P_{FWE} < 0.001$, left: -14, 10 -10, $t(75) = 4.91$, $P_{FWE} < 0.001$). Notably, while we found no association between SA and feedback processing, we were able to replicate the previously observed association between SA and amygdala hyperactivity during social decision-making in the LL group (SA scores correlated with right amygdala activity for risky decision human > risky decision computer: $r(35) = 0.41$, $P = 0.01$; risky decision human > safe decision human: $r(35) = 0.44$, $P = 0.007$). For whole-brain task effects, see **Table 1** and **Table 2**.

Importantly, however, neither amygdala activation during the decision or feedback stage nor the accuracy of decoding risky vs. safe decisions based on amygdala activation patterns significantly differed between HL and LL participants. Conversely, we observed significant differences in striatal responses to the feedback videos: HL participants showed significantly smaller NAcc responses to human (vs. computer) feedback than LL individuals (14, 14, -10, $t(74) = 3.07$, $P_{FWE} = 0.02$). Again, the group difference was specific for negative feedback (14, 14, -10, $t(74) = 3.21$, $P_{FWE} = 0.01$; see **Fig. 3B**), whereas no significant group effects were observed for responses to positive feedback. Post-hoc tests revealed increased NAcc responsiveness to negative human feedback compared to the computer feedback in LL participants ($t(36) = 2.59$, $P_{cor} = 0.03$, $d = 0.53$), while HL participants exhibited the opposite response pattern ($t(38) = -1.96$, $P_{cor} = 0.12$). In line with the behavioral results, further explorative post-hoc tests indicated that group differences were based on a significantly enhanced NAcc responsiveness to the negative computer feedback in HL participants (HL vs. LL: $t(74) = 2.80$, $P_{cor} = 0.01$, $d = 0.62$), whereas group differences showed the opposite

tendency for responses to negative human feedback ($t(74) = -0.98$, $P_{cor} = 0.64$). No further group differences in brain activity were observed.

Exploratory gPPI analyses of the negative feedback condition with the NAcc serving as seed region indicated enhanced functional connectivity of the left NAcc with a cluster including the hippocampus in HL compared to LL participants (-14, -22, -14, $k = 73$, $t(74) = 5.38$, $P_{FWE} = 0.049$ on cluster level; see **Fig. 4**). Again, post-hoc tests revealed an opposing pattern between groups when receiving negative human (vs. computer) feedback: enhanced connectivity in HL participants ($t(38) = 3.06$, $P_{cor} = 0.01$, $d = 0.63$) but reduced connectivity in LL participants ($t(36) = -4.93$, $P_{cor} < 0.001$, $d = -1.15$). Two further post-hoc comparisons again revealed differences between groups for negative computer feedback as functional connectivity was significantly reduced in HL participants (HL vs. LL: $t(74) = -4.62$, $P_{cor} < 0.001$, $d = 1.06$), whereas the involvement of a human partner reversed this pattern with significantly increased functional connectivity in HL participants (HL vs. LL: $t(74) = 2.40$, $P_{cor} = 0.04$, $d = 0.55$). Interestingly, NAcc-hippocampus connectivity not only correlated with NAcc responses to negative human feedback (contrasted with negative computer feedback: $r(74) = -0.33$, $P = 0.004$, i.e., increased connectivity was associated with reduced neural reactivity), but also with pleasantness ratings of negative feedback videos ($r(74) = 0.23$, $P = 0.04$, see **Fig. 4**). The correlation between NAcc activity and negative feedback ratings was similar, but failed to reach significance ($r(74) = -0.20$, $P = 0.09$).

Bayesian analyses

Bayesian analyses revealed moderate evidence for the absence of group differences in variables that have previously been associated with SA (cf. Schultz et al. (2019)), with our data being at least three times more likely under the null hypothesis (H0: no differences between groups) than under the alternative hypothesis (HL differ from LL participants in any

direction). Specifically, Bayesian t-tests revealed moderate evidence that HL participants indeed did not differ from LL participants regarding the pleasantness ratings of positive human feedback as our data were found to be almost four times more likely under the H0 than under the alternative hypothesis (Bayes factor (BF_{10}) = 0.25, median effect size = 0.08, 95 % credible interval: [-0.32, 0.49]).

Likewise, Bayesian analyses revealed moderate evidence that groups showed equal reward-associated brain activity in response to positive human feedback (left NAcc: BF_{10} = 0.25, median effect size = 0.07, 95 % credible interval: [-0.35, 0.49]; for the right NAcc the evidence is inconclusive: BF_{10} = 0.43, median effect size = 0.23, 95 % credible interval: [-0.19, 0.66]) and moderate evidence in favor of the H0 for amygdala reactivity to human feedback (left: BF_{10} = 0.24, median effect size = -0.004, 95 % credible interval: [-0.42, 0.41]; right: BF_{10} = 0.24, median effect size ≈ 0.00, 95 % credible interval: [-0.42, 0.42]). The same pattern of results was observed for amygdala activation during the decision stage of the social gambling task as our data were up to four times more likely under the assumption of comparable activation between groups (H0) than under the alternative hypothesis (left amygdala activation for risky decisions with a human partner compared to a computer partner: BF_{10} = 0.24, median effect size = 0.03, 95 % credible interval: [-0.39, 0.45]; left amygdala activation for risky decisions with a human partner contrasted with safe decisions in trials with a human partner: BF_{10} = 0.33, median effect size = -0.17, 95 % credible interval: [-0.61, 0.25]; right: BF_{10} = 0.24, median effect size = -0.01, 95 % credible interval: [-0.43, 0.41]). For right amygdala activation, there was insufficient evidence to draw a conclusion for or against the hypothesis that groups exhibit equal responsiveness to risky decisions involving a human partner (contrasted with the computer; BF_{10} = 0.50, median effect size = 0.26, 95 % credible interval: [-0.16, 0.70]). However, descriptive analyses revealed an opposing response pattern in HL participants to what has been expected due to increased SA symptoms: while LL participants showed slightly enhanced amygdala activation (mean parameter estimates ± SD: 0.25 ± 1.06), amygdala activation was reduced in HL participants

609 (mean parameter estimates ± SD: -0.02 ± 0.68; cf. **Fig. 3A**). Likewise, no evidence for any of
610 the hypotheses (null or alternative hypothesis) was observed for the subjective value of
611 engaging in social situations (BF_{10} = 0.57, median effect size = -0.29, 95 % credible interval =
612 [-0.74, 0.15]). Again, descriptive analyses revealed enhanced values of social engagement in
613 HL compared to LL participants, which is contrary to the previously reported negative
614 association with SA (see inlay of **Fig. 2B** and cf. Schultz et al. (2019)).

615 Regarding the invested money during the virtual auction task, Bayesian analyses provided
616 moderate evidence for comparable investments between groups to avoid negative human
617 feedback (BF_{10} = 0.33, median effect size = 0.17, 95 % credible interval = [-0.23, 0.59]) or to
618 receive positive human feedback (BF_{10} = 0.33, median effect size = 0.18, 95 % credible
619 interval = [-0.23, 0.59]).

620

621 **Interactions of loneliness with SA**

622 To summarize, although HL individuals reported higher SA scores, loneliness was not
623 associated with behavioral and neural correlates which have been previously found to be
624 affected by SA and which could be partially replicated in LL participants. We thus explored
625 whether SA-related findings differed significantly between HL and LL participants. Indeed,
626 moderation analyses revealed that SA-related effects on amygdala activation during social
627 decision-making were significantly different for HL compared to LL participants (interaction of
628 SA with group for right amygdala activation during risky decisions with a human partner
629 compared to safe decisions with a human partner: β = -0.88, $t(70)$ = -3.02, P = 0.004, 95 %
630 CI: [-1.47, -0.30]; for right amygdala activation during risky decisions with a human partner
631 compared to risky decisions with the computer partner: β = -0.63, $t(70)$ = -2.16, P = 0.03, 95
632 % CI: [-1.20, -0.05]; see **Fig. 5A** and **Fig. 5B**). As already reported (see fMRI results), SA
633 was positively associated with the average activation across all voxels of the right amygdala

for risky decisions involving a human partner (compared to safe decisions involving a human partner: β = 0.63, *P* = 0.007, 95 % CI: [0.18, 1.08]; compared to risky decisions involving the computer: β = 0.69, *P* = 0.003, 95 % CI: [0.25, 1.14]) in LL participants. Conversely, this association vanished in the HL group (risky decisions involving a human partner vs. safe decisions involving a human partner: β = -0.26, *P* = 0.17, 95 % CI: [-0.63, 0.11]; risky decisions involving a human partner vs. risky decisions involving a computer partner: β = 0.07, *P* = 0.72, 95 % CI: [-0.30, 0.43]). Moreover, moderation analyses indicated that the association of SA with the subjective values of engaging in social situations might be altered in HL participants (interaction of SA with group: β = 0.57, *t*(67) = 1.84 *P* = 0.07, 95 % CI: [-0.05, 1.18]; see **Fig. 5C**). As such, the reported non-significant negative association of SA with the social engagement in the LL group (β = -0.17, *P* = 0.48, 95 % CI: [-0.64, 0.30]; see also behavioral results) was reversed in the HL group (β = 0.40, *P* = 0.049, 95 % CI: [0.002, 0.80]). Thus, higher SA symptomatology was significantly associated with increased subjective values of engaging in social situations for participants suffering from loneliness.

We then probed whether the differences between HL and LL participants were based on increased SA score in HL participants or whether loneliness effects on the processing of negative feedback differed for participants with high or low SA scores. Importantly, the observed effects of loneliness (HL vs. LL) on NAcc responsiveness to negative human feedback (vs. negative computer feedback) and on the NAcc-hippocampal functional connectivity while receiving negative feedback remained significant after including SA scores as covariate in the regression models (*P*s < 0.01 for all direct effects of group after including SA). Furthermore, no significant interactions between group and SA were observed, indicating that an altered processing of negative feedback in HL participants was not enhanced or diminished by increased SA symptomatology. Finally, we explored whether the altered feedback processing in HL participants was driven by increased SA by calculating mediation analyses with SA scores as potential mediator. Results revealed that none of the reported group effects was driven by SA. Conversely, analyses showed a significant

suppressor effect of SA on the relationship between group and NAcc responses (indirect effect of group on NAcc activity via SA: β = 0.14, SE = 0.10, 95 % CI: [0.005, 0.40]). Thus, the absolute height of the group effect even increased after including SA as mediator (effect of group without taking SA into account: β = -0.69, SE = 0.22, 95 % CI: [-1.12, -0.26]; with SA as mediator: β = -0.83, SE = 0.23, 95 % CI: [-1.28, -0.38]; for NAcc-hippocampal functional connectivity and pleasantness ratings of negative human vs. computer feedback 95 % CIs included zero for the SA mediator effect (i.e., the indirect effect of group via SA)).

Effects of further confounding variables

Groups differed significantly regarding psychiatric symptoms (cf. Lieberz et al. (2021)). In addition to increased SA symptomatology, HL participants reported more depressive symptoms ($t(50.89) = 4.15$, $P < 0.001$, $d = 0.92$; mean BDI score ± SD in HL: 6.62 ± 6.76; LL: 2.03 ± 2.31) and more severe childhood maltreatment ($t(80) = 2.38$, $P = 0.02$, $d = 0.53$; mean CTQ score ± SD in HL: 38.86 ± 10.28; LL: 31.90 ± 15.76). Importantly, as reported for SA, the observed effects of loneliness (HL vs. LL) on NAcc responsiveness to negative human feedback remained significant after including the depression or childhood maltreatment as covariates in the regression models (Ps < 0.01 for all direct effects of group after including the potential confounding variables). Likewise, loneliness effects on NAcc-hippocampal functional connectivity while receiving negative human feedback were found to be robust (all direct effects of group after including the potential confounding variables Ps < 0.0001). Mediation and moderation analyses indicated that none of the reported group effects was mediated or moderated by confounding psychiatric symptoms (the 95 % CI of all tested indirect effects included zero and all interaction effects of group with the potential moderator $P > 0.05$).

Discussion

The current study sought to investigate shared and distinct behavioral and neural response patterns underlying SA and loneliness. While we were able to replicate previously reported task effects and SA-related amygdala hyperactivation during social decision-making (cf. Schultz et al. (2019)), our results revealed that a previously observed neurocircuitry underlying avoidance behavior in SA is not evident in lonely individuals. HL participants differed from LL participants neither in the subjective value of engaging in social situations nor in neural responses to social decision-making and positive social feedback. Moreover, the association of SA symptomatology with increased amygdala activation during social decision-making vanished in HL participants. Conversely, the previously reported positive association of SA with reduced subjective values of engaging in social situations was even reversed in HL participants. Further explorative analyses indicated that HL participants showed an altered responsiveness to negative computer feedback as evident in reduced pleasantness ratings and increased striatal activity, which was normalized when negative feedback was provided by a human partner. Moreover, striatal-hippocampal functional connectivity in HL participants, which was diminished while receiving negative computer feedback, was significantly increased during negative social feedback.

Our results indicate that neural and behavioral correlates of loneliness differ from a socially avoidant phenotype associated with SA. Loneliness did not significantly correlate with behavioral tendencies to withdraw from social interactions in the current study. Human and animal research have consistently shown that the amygdala is crucially involved in the processing of threat-related stimuli and hyperactivation of the amygdala is known as a core mechanism underlying anxiety disorders (Phelps & LeDoux, 2005; Etkin & Wager, 2007). Moreover, amygdala habituation to threat-related stimuli and amygdala connectivity with prefrontal regions predict subsequent avoidance behavior (Björkstrand et al., 2020; Lisk et

al., 2020; Mao et al., 2020). Likewise, we have previously found that amygdala activation during decisions in the social gambling task increases with SA symptomatology and negatively correlates with the subjective value to engage in social situations (Schultz et al., 2019). By contrast, the subjective value of engaging in a social situation did not differ between HL and LL participants and Bayesian analyses revealed evidence for comparable amygdala activation during the decision and feedback stages. Moreover, the link between amygdala activation during social decision-making and SA symptoms differed significantly between HL and LL participants, thus providing further support for the heterogeneity in clinical phenotypes and underlying biotypes of SA (Spokas & Cardaciotto, 2014; Williams, 2017). In line with our findings, neuroanatomical correlates of social avoidance behavior were previously found to be unaffected by loneliness (Tian et al., 2016). This notion is consistent with etiological theories that highlight maladaptive social cognitions in the development and maintenance of loneliness (Spithoven et al., 2017; Cacioppo & Cacioppo, 2018). Likewise, cognitive-behavioral interventions were found to be more effective in targeting social biases than social skill trainings (Masi et al., 2011; Veronese et al., 2020). There is preliminary evidence that established cognitive-behavioral treatments targeting SA concurrently decrease feelings of loneliness and vice versa (Alfano et al., 2009; Suveg et al., 2017; Haslam et al., 2019; Kall et al., 2021; O'Day et al., 2021), but our findings of distinct behavioral and neural substrates suggest that loneliness-adjusted protocols might improve therapeutic outcomes.

Moreover, our explorative results provide new insights into the neural pathways underlying loneliness. Unexpectedly, striatal activity during negative social feedback was reduced while pleasantness ratings were increased in HL participants. Notably, activation of the NAcc is associated with goal-directed approach and avoidance behavior and involved in avoiding social punishment (Kohls et al., 2013; Damiano et al., 2015; Floresco, 2015). Furthermore, our results are in line with parcellation studies highlighting specific roles of the ventral-caudal NAcc shell and the rostral, core-like NAcc. The former has been associated with reward

anticipation and reward processing, while activation of the latter may also reflect the processing of negative events (Baliki et al., 2013; Xia et al., 2017; Oldham et al., 2018). Concordantly, the observed group differences in response to negative feedback were restricted to rostral, core-like parts of the NAcc, whereas positive feedback activated both rostral and caudal parts of the NAcc across groups. As HL participants rated the negative social feedback videos as more pleasant than the negative computer feedback, reduced core-like NAcc responses to negative social feedback might thus reflect reduced tendencies to avoid this negative social feedback. Conversely, the opposite pattern of results was observed for LL participants. Furthermore, the enhanced functional coupling of the NAcc with a hippocampal cluster that correlated with individual pleasantness ratings is in line with the involvement of this neural circuit in hedonic processing (Yang et al., 2020) and might reflect the rewarding experience of a social feedback for socially deprived individuals (Tomova et al., 2020). As such, our results indicate that HL participants might be more affected by negative events compared to LL participants. The involvement of another human, however, might attenuate this bias. Nevertheless, we have recently found a compromised neural integration of social information in HL participants evident in various brain regions including the NAcc (Lieberz et al., 2021). Furthermore, loneliness has been associated with a reduced recognition of negative vocal expressions (Morningstar et al., 2020). Thus, the reduced NAcc activity might also reflect diminished differentiation between positive and negative feedback, resulting in a dysregulated reward system responsiveness to negative social stimuli as observed for the NAcc-hippocampus connectivity. However, inference about cognitive processes from neural activation should always be drawn with restraint (Poldrack, 2006) and results regarding biased emotion recognition in loneliness are inconclusive (Spithoven et al., 2017). Future studies are warranted to further investigate the impact of loneliness on the processing of negative events in general and on the processing of negative social feedback in particular. For instance, implementing representational similarity analyses and incorporating multimodal data might help to understand how negative social feedback is

765 represented in HL participants, how its processing contributes to future behavior and whether
766 its neural representation differs from LL individuals or from patients suffering from SA.

767 Interestingly, differences between HL and LL participants were restricted to behavioral and
768 neural responses to negative social feedback, whereas Bayesian analyses revealed
769 evidence for a comparable responsiveness to positive social feedback between groups.
770 Conversely, SA has been consistently found to affect the processing of social rewards
771 (Sripada et al., 2013; Richey et al., 2014; Richey et al., 2017; Schultz et al., 2019). Previous
772 studies point to various negative effects of loneliness on the processing of positive social
773 interactions (Cacioppo et al., 2009; Silva et al., 2017; Lieberz et al., 2021), but findings about
774 the association between loneliness and NAcc reactivity to positive social stimuli are mixed.
775 The involvement of the NAcc in loneliness might be context-dependent, with feelings of
776 social isolation promoting the hedonic experience of positive social stimuli in an acute stage
777 (Tomova et al., 2020), which may be different from chronic loneliness (Saporta et al., 2021).
778 Similarly, lonely individuals might experience a social stimulus as more rewarding only if the
779 stimulus is already familiar (e.g., a romantic partner and not a stranger (Inagaki et al., 2016)).
780 Along these lines, a recent study found no relationship of loneliness with striatal
781 responsiveness to pictures depicting strangers during positive social interactions (D'Agostino
782 et al., 2018). Nevertheless, in our task design positive feedback was always coupled with
783 monetary gains. Thus, differences regarding positive social feedback might have been
784 obfuscated by the rewarding experience of earning money as evident in enhanced striatal
785 responsiveness to positive feedback, irrespective of the partner providing the feedback. Both
786 external (e.g., passive viewing vs. being involved in positive social interactions) and internal
787 factors (e.g., state vs. chronic feelings of social isolation) may influence the association of
788 loneliness with social reward processing.

789 Moreover, given the quasi-experimental, cross-sectional design of our study, our findings do
790 not allow casual inferences about the relationship of loneliness and social feedback

processing. Additionally, analyses indicate that the observed associations with loneliness were not driven by psychiatric symptoms that were also more pronounced in HL individuals. However, our study specifically focused on high-lonely healthy individuals who may represent a resilient subsample of the population because they did not develop acute psychiatric disorders. Thus, clinical studies with psychiatric patients are warranted to uncover the direction of the observed associative relationships and to further disentangle shared and distinct mechanisms underlying loneliness and psychopathology. Likewise, we cannot exclude the possibility that the LL group may also represent a special, hyper-social group, that differs from the average population. Nevertheless, previous studies indicated that the intensity of loneliness matters mostly for individuals with high loneliness, whereas differences in the experience of loneliness between low and medium lonely individuals had no effect on loneliness-related hypervigilance for social threats (Qualter et al., 2013). While it thus seems unlikely that the inclusion of an intermediate group with average loneliness scores would change the direction of the observed group differences, it might still be of great interest for future studies to investigate clinically relevant cutoff points in either direction. This way, research might help to identify individuals who are at high risk for mental and physical health problems due to high loneliness and in turn to characterize protective mechanisms of highly social individuals that might prevent psychiatric disorders.

Collectively, the current results suggest that loneliness and SA are distinct constructs with specific behavioral and neural substrates. Along these lines, interventions targeting loneliness-specific cognitive biases may be more effective in reducing loneliness than cognitive-behavioral therapies focused on reducing avoidance behavior.

References

Alfano, C. A., Pina, A. A., Villalta, I. K., Beidel, D. C., Ammerman, R. T.,Crosby, L. E. (2009). Mediators and moderators of outcome in the behavioral treatment of childhood social phobia. Journal of the American Academy of Child and Adolescent Psychiatry, 48(9), 945-953.

Baliki, M. N. et al. (2013). Parceling human accumbens into putative core and shell dissociates encoding of values for reward and pain. Journal of Neuroscience, 33(41), 16383-16393.

Beck, A., Steer, R. A.,Brown, G. K. (1996). Beck Depression Inventory-II. San Antonio, TX: Psychological Corporation.

Bernstein, D. P. et al. (1994). Initial Reliability and Validity of a New Retrospective Measure of Child Abuse and Neglect. American Journal of Psychiatry, 151(8), 1132-1136.

Björkstrand, J. et al. (2020). Decrease in amygdala activity during repeated exposure to spider images predicts avoidance behavior in spider fearful individuals. Translational Psychiatry, 10(1).

Bruce, L. D., Wu, J. S., Lustig, S. L., Russell, D. W.,Nemecek, D. A. (2019). Loneliness in the United States: a 2018 national panel survey of demographic, structural, cognitive, and behavioral characteristics. American Journal of Health Promotion, 33(8), 1123-1133.

Bruhl, A. B., Delsignore, A., Komossa, K.,Weidt, S. (2014). Neuroimaging in social anxiety disorder-a meta-analytic review resulting in a new neurofunctional model. Neuroscience and Biobehavioral Reviews, 47, 260-280.

Cacioppo, J. T.,Cacioppo, S. (2018). Chapter Three - Loneliness in the Modern Age: An Evolutionary Theory of Loneliness (ETL). In: Advances in Experimental Social Psychology (J. M. Olson (ed), (Vol. 58, pp. 127-197). Cambridge, MA: Academic Press.

839 Cacioppo, J. T., Hawkley, L. C.,Thisted, R. A. (2010). Perceived social isolation makes me
840 sad: 5-year cross-lagged analyses of loneliness and depressive symptomatology in
841 the Chicago Health, Aging, and Social Relations Study. Psychology and Aging, 25(2),
842 453-463.
843 Cacioppo, J. T., Norris, C. J., Decety, J., Monteleone, G.,Nusbaum, H. (2009). In the Eye of
844 the Beholder: Individual Differences in Perceived Social Isolation Predict Regional
845 Brain Activation to Social Stimuli. Journal of Cognitive Neuroscience, 21(1), 83-92.
846 Cho, J. W., Korchmaros, A., Vogelstein, J. T., Milham, M. P.,Xu, T. (2020). Impact of
847 concatenating fMRI data on reliability for functional connectomics. Neuroimage, 226,
848 117549.
849 Clark, D. M.,Wells, A. (1995). A Cognitive Model of Social Phobia. In: Social phobia:
850 Diagnosis, assessment, and treatment (R. G. Heimberg, M. R. Liebowitz, D. A. Hope,
851 & F. R. Schneider (eds), (pp. 69-94). New York, NY: The Guilford Press.
852 D'Agostino, A. E., Kattan, D.,Canli, T. (2018). An fMRI study of loneliness in younger and
853 older adults. Social Neuroscience, 1-13.
854 Damiano, C. R. et al. (2015). Neural mechanisms of negative reinforcement in children and
855 adolescents with autism spectrum disorders. Journal of Neurodevelopmental
856 Disorders, 7, 12.
857 Danneel, S. et al. (2019). Internalizing Problems in Adolescence: Linking Loneliness, Social
858 Anxiety Symptoms, and Depressive Symptoms Over Time. Journal of Abnormal Child
859 Psychology, 47(10), 1691-1705.
860 Etkin, A.,Wager, T. D. (2007). Functional Neuroimaging of Anxiety: A Meta-Analysis of
861 Emotional Processing in PTSD, Social Anxiety Disorder, and Specific Phobia.
862 American Journal of Psychiatry, 164(10), 1476-1488.
863 Faul, F., Erdfelder, E., Lang, A.-G.,Buchner, A. (2007). G*Power 3: A flexible statistical
864 power analysis program for the social, behavioral, and biomedical sciences. Behavior
865 Research Methods, 39(2), 175-191.

866 Floresco, S. B. (2015). The nucleus accumbens: an interface between cognition, emotion,
867 and action. Annual Review of Psychology, 66, 25-52.
868 Galea, S., Merchant, R. M.,Lurie, N. (2020). The Mental Health Consequences of COVID-19
869 and Physical Distancing: The Need for Prevention and Early Intervention. JAMA
870 Intern Med, 180(6), 817-818.
871 Haslam, C. et al. (2019). GROUPS 4 HEALTH reduces loneliness and social anxiety in
872 adults with psychological distress: findings from a randomized controlled trial. Journal
873 of Consulting and Clinical Psychology, 87(9), 787-801.
874 Hayes, A. F. (2017). Introduction To Mediation, Moderation, And Conditional Process
875 Analysis: A Regression-Based Approach. New York, NY: Guilford publications.
876 Hebart, M. N., Gorgen, K.,Haynes, J. D. (2014). The Decoding Toolbox (TDT): a versatile
877 software package for multivariate analyses of functional imaging data. Frontiers in
878 Neuroinformatics, 8, 88.
879 Heinrich, L. M.,Gullone, E. (2006). The clinical significance of loneliness: A literature review.
880 Clinical Psychology Review, 26(6), 695-718.
881 Holt-Lunstad, J., Smith, T. B.,Layton, J. B. (2010). Social relationships and mortality risk: A
882 meta-analytic review. PLoS Medicine, 7(7), e1000316.
883 Inagaki, T. K. et al. (2016). Yearning for connection? Loneliness is associated with increased
884 ventral striatum activity to close others. Social Cognitive and Affective Neuroscience,
885 11(7), 1096-1101.
886 JASP Team. (2020). JASP (Version 0.14.1)[Computer software]. https://jasp-stats.org/.
887 Retrieved from https://jasp-stats.org/
888 Jeste, D. V., Lee, E. E.,Cacioppo, S. (2020). Battling the Modern Behavioral Epidemic of
889 Loneliness: Suggestions for Research and Interventions. JAMA Psychiatry, 77(6),
890 553-554.

Kall, A. et al. (2021). Therapist-Guided Internet-Based Treatments for Loneliness: A Randomized Controlled Three-Arm Trial Comparing Cognitive Behavioral Therapy and Interpersonal Psychotherapy. Psychotherapy and Psychosomatics, 1-8.

Kashdan, T. B.,Collins, R. L. (2010). Social anxiety and the experience of positive emotion and anger in everyday life: an ecological momentary assessment approach. Anxiety Stress Coping, 23(3), 259-272.

Kaulard, K., Cunningham, D. W., Bulthoff, H. H.,Wallraven, C. (2012). The MPI facial expression database--a validated database of emotional and conversational facial expressions. PloS One, 7(3), e32321.

Keysers, C., Gazzola, V.,Wagenmakers, E. J. (2020). Using Bayes factor hypothesis testing in neuroscience to establish evidence of absence. Nature Neuroscience, 23(7), 788-799.

Kohls, G. et al. (2013). The nucleus accumbens is involved in both the pursuit of social reward and the avoidance of social punishment. Neuropsychologia, 51(11), 2062-2069.

Lam, J. A. et al. (2021). Neurobiology of loneliness: a systematic review. Neuropsychopharmacology.

Lieberz, J. et al. (2021). Loneliness and the Social Brain: How Perceived Social Isolation Impairs Human Interactions. Adv Sci (Weinh), e2102076.

Liebowitz, M. R. (1987). Social phobia. Modern Problems of Pharmacopsychiatry, 22, 141-173.

Lim, M. H., Rodebaugh, T. L., Zyphur, M. J.,Gleeson, J. F. (2016). Loneliness over time: The crucial role of social anxiety. Journal of Abnormal Psychology, 125(5), 620-630.

Lisk, S., Kadosh, K. C., Zich, C., Haller, S. P.,Lau, J. Y. (2020). Training negative connectivity patterns between the dorsolateral prefrontal cortex and amygdala through fMRI-based neurofeedback to target adolescent socially-avoidant behaviour. Behaviour Research and Therapy, 135, 103760.

Maes, M. et al. (2019). Loneliness and social anxiety across childhood and adolescence: Multilevel meta-analyses of cross-sectional and longitudinal associations. Developmental Psychology, 55(7), 1548-1564.

Maldjian, J. A., Laurienti, P. J.,Burdette, J. H. (2004). Precentral gyrus discrepancy in electronic versions of the Talairach atlas. Neuroimage, 21(1), 450-455.

Maldjian, J. A., Laurienti, P. J., Kraft, R. A.,Burdette, J. H. (2003). An automated method for neuroanatomic and cytoarchitectonic atlas-based interrogation of fMRI data sets. Neuroimage, 19(3), 1233-1239.

Mao, Y., Zuo, X. N., Ding, C.,Qiu, J. (2020). OFC and its connectivity with amygdala as predictors for future social anxiety in adolescents. Developmental Cognitive Neuroscience, 44, 100804.

Masi, C. M., Chen, H. Y., Hawkley, L. C.,Cacioppo, J. T. (2011). A meta-analysis of interventions to reduce loneliness. Personality and Social Psychology Review, 15(3), 219-266.

Mihalopoulos, C. et al. (2020). The economic costs of loneliness: A review of cost-of-illness and economic evaluation studies. Social Psychiatry and Psychiatric Epidemiology, 55, 823-836.

Morningstar, M., Nowland, R., Dirks, M. A.,Qualter, P. (2020). Loneliness and the recognition of vocal socioemotional expressions in adolescence. Cognition & Emotion, 34(5), 970-976.

O'Day, E. B., Butler, R. M., Morrison, A. S., Goldin, P. R., Gross, J. J.,Heimberg, R. G. (2021). Reductions in social anxiety during treatment predict lower levels of loneliness during follow-up among individuals with social anxiety disorder. Journal of Anxiety Disorders, 78, 102362.

Oldham, S., Murawski, C., Fornito, A., Youssef, G., Yucel, M.,Lorenzetti, V. (2018). The anticipation and outcome phases of reward and loss processing: A neuroimaging

meta-analysis of the monetary incentive delay task. Human Brain Mapping, 39(8), 3398-3418.

Peplau, L. A.,Caldwell, M. A. (1978). Loneliness: A cognitive analysis. Essence, 2(4), 207-220.

Phelps, E. A.,LeDoux, J. E. (2005). Contributions of the Amygdala to Emotion Processing: From Animal Models to Human Behavior. Neuron, 48(2), 175-187.

Poldrack, R. A. (2006). Can cognitive processes be inferred from neuroimaging data? Trends in Cognitive Sciences, 10(2), 59-63.

Porter, E.,Chambless, D. L. (2014). Shying away from a good thing: social anxiety in romantic relationships. Journal of Clinical Psychology, 70(6), 546-561.

Quadt, L., Esposito, G., Critchley, H. D.,Garfinkel, S. N. (2020). Brain-body interactions underlying the association of loneliness with mental and physical health. Neuroscience and Biobehavioral Reviews.

Qualter, P. et al. (2013). Investigating hypervigilance for social threat of lonely children. Journal of Abnormal Child Psychology, 41(2), 325-338.

Rapee, R. M., Peters, L., Carpenter, L.,Gaston, J. E. (2015). The Yin and Yang of support from significant others: Influence of general social support and partner support of avoidance in the context of treatment for social anxiety disorder. Behaviour Research and Therapy, 69, 40-47.

Richey, J. A. et al. (2017). Spatiotemporal dissociation of brain activity underlying threat and reward in social anxiety disorder. Social Cognitive and Affective Neuroscience, 12(1), 81-94.

Richey, J. A. et al. (2014). Common and distinct neural features of social and non-social reward processing in autism and social anxiety disorder. Social Cognitive and Affective Neuroscience, 9(3), 367-377.

969 Rodebaugh, T. L., Lim, M. H., Shumaker, E. A., Levinson, C. A.,Thompson, T. (2015). Social
970 Anxiety and Friendship Quality over Time. Cognitive Behaviour Therapy, 44(6), 502-
971 511.
972 Ruff, C. C.,Fehr, E. (2014). The neurobiology of rewards and values in social decision
973 making. Nature Reviews: Neuroscience, 15(8), 549-562.
974 Russell, D., Peplau, L. A.,Cutrona, C. E. (1980). The Revised UCLA Loneliness Scale:
975 Concurrent and Discriminant Validity Evidence. Journal of Personality and Social
976 Psychology, 39(3), 472-480.
977 Saporta, N., Scheele, D., Lieberz, J., Stuhr-Wulff, F., Hurlemann, R.,Shamay-Tsoory, S. G.
978 (2021). Opposing Association of Situational and Chronic Loneliness with
979 Interpersonal Distance. Brain Sciences, 11(9), 1135.
980 Schultz, J. et al. (2019). A human subcortical network underlying social avoidance revealed
981 by risky economic choices. Elife, 8, e45249.
982 Shao, R. et al. (2019). Loneliness and depression dissociated on parietal-centered networks
983 in cognitive and resting states. Psychological Medicine, 1-11.
984 Sheehan, D. V. et al. (1998). The Mini-International Neuropsychiatric Interview (M.I.N.I.): The
985 Development and Validation of a Structured Diagnostic Psychiatric Interview for
986 DSM-IV and ICD-10. Journal of Clinical Psychiatry, 59(Suppl 20), 22-33.
987 Silva, H. D. et al. (2017). Bonding Pictures: Affective Ratings Are Specifically Associated to
988 Loneliness But Not to Empathy. Frontiers in Psychology, 8, 1136.
989 Spithoven, A. W. M., Bijttebier, P.,Goossens, L. (2017). It is all in their mind: A review on
990 information processing bias in lonely individuals. Clinical Psychology Review, 58, 97-
991 114.
992 Spokas, M. E.,Cardaciotto, L. (2014). Heterogeneity Within Social Anxiety Disorder. In: The
993 Wiley Blackwell Handbook of Social Anxiety Disorder (pp. 247-267).

994 Sripada, C., Angstadt, M., Liberzon, I., McCabe, K.,Phan, K. L. (2013). Aberrant reward
995 center response to partner reputation during a social exchange game in generalized
996 social phobia. Depression and Anxiety, 30(4), 353-361.
997 Suveg, C., Kingery, J. N., Davis, M., Jones, A., Whitehead, M.,Jacob, M. L. (2017). Still
998 lonely: Social adjustment of youth with and without social anxiety disorder following
999 cognitive behavioral therapy. Journal of Anxiety Disorders, 52, 72-78.
1000 Teo, A. R., Lerrigo, R.,Rogers, M. A. (2013). The role of social isolation in social anxiety
1001 disorder: a systematic review and meta-analysis. Journal of Anxiety Disorders, 27(4),
1002 353-364.
1003 Tian, X., Hou, X., Wang, K., Wei, D.,Qiu, J. (2016). Neuroanatomical correlates of individual
1004 differences in social anxiety in a non-clinical population. Social Neuroscience, 11(4),
1005 424-437.
1006 Tomova, L. et al. (2020). Acute social isolation evokes midbrain craving responses similar to
1007 hunger. Nature Neuroscience, 23, 1597-1605.
1008 Veronese, N. et al. (2020). Interventions for reducing loneliness: An umbrella review of
1009 intervention studies. Health Soc Care Community, 00, 1-8.
1010 Vindegaard, N.,Benros, M. E. (2020). COVID-19 pandemic and mental health consequences:
1011 Systematic review of the current evidence. Brain, Behavior, and Immunity, 89, 531-
1012 542.
1013 Williams, L. M. (2017). Defining biotypes for depression and anxiety based on large-scale
1014 circuit dysfunction: a theoretical review of the evidence and future directions for
1015 clinical translation. Depression and Anxiety, 34(1), 9-24.
1016 Xia, X. et al. (2017). Multimodal connectivity-based parcellation reveals a shell-core
1017 dichotomy of the human nucleus accumbens. Human Brain Mapping, 38(8), 3878-
1018 3898.

1019 Yang, A. K., Mendoza, J. A., Lafferty, C. K., Lacroix, F.,Britt, J. P. (2020). Hippocampal Input
1020 to the Nucleus Accumbens Shell Enhances Food Palatability. Biological Psychiatry,
1021 87(7), 597-608.

Figure Legends

Fig. 1. Social gambling task. The social gambling task included a human (**A**) and a computer (**B**) condition and each trial consisted of a decision and a feedback stage. During the decision phase, participants could choose a risky or a safe option (a uniformly distributed random fixed payoff ranging from 0 to 3 € in steps of 50 cents). If participants chose the risky option and won the trial, a positive feedback video of the partner was shown and the participant got 3 €. If participants lost the trial, they received no payoff and a negative feedback video was presented. The human feedback video displayed the virtual human partner expressing either admiration (participants won) or condescension (participant lost). In the computer control condition, the feedback was given by a video of a checkmark (participant won) or a cross (participant lost). If participants chose the safe option, a sentence confirmed the payoff. During functional magnetic resonance imaging, the partner was indicated by the name of the virtual human partner or the word “computer” only. (**C**) The four virtual human partners with neutral facial expression. (**D**) One of the partners with neutral, admiring, and condescending facial expressions (left to right). The admiring and condescending expressions were presented as videos during the feedback stage. See also Figure 1 of Schultz et al. (2019).

Fig. 2. Behavioral results of the decision and feedback phase of the social gambling task. (**A**) Participants with a high loneliness score (HL) showed significantly increased social anxiety scores as assessed with the Liebowitz Social Anxiety Scale. **(B)** The proportion of safe decisions during the social gambling task increased with higher payoffs offered in those safe decisions (main effect of offered payoff for the behavioral task: $F(2.95,236.14) = 183.77$, $P < 0.001$, $\eta_p^2 = 0.70$; functional magnetic resonance imaging task: $F(2,158) = 185.43$, $P < 0.001$, $\eta_p^2 = 0.70$; example data of the behavioral task from one HL participant are presented). As presented in the inlay, HL participants did not significantly differ from participants with low loneliness scores (LL) with regard to the subjective value of engaging in a social situation (i.e., CE50, the payoff offered in the safe option associated with 50% of safe decisions; $t(47.81) = 1.42$, $P = 0.16$, Bayes factor (BF_{10}) = 0.57). (**C**) By contrast, groups significantly differed in their pleasantness ratings of the negative feedback videos. Compared to the negative computer feedback video, HL participants rated the negative human feedback video as more pleasant, whereas LL participants showed the opposite pattern of ratings. No differences between groups were observed for positive feedback. Each marker in (A) represents the mean of 8 trials. Bars represent group means. Error bars indicate standard errors of the mean. Abbreviations: n.s., not significant. * $P < 0.05$, ** $P < 0.01$.

Fig. 3. Neural activation during the social gambling task. (**A**) Amygdala activity was significantly enhanced during the decision phase of the social gambling task when participants chose the risky option with a human partner compared to the computer partner (right: 22, -6, -12, $t(73) = 4.58$, $P_{FWE} = 0.002$; left: -22, -8, -12, $t(73) = 4.23$, $P_{FWE} = 0.006$). In line with the behavioral results, no group differences in neural activity were observed during the decision phase. (**B**) During the feedback stage, participants with high loneliness scores (HL) showed attenuated nucleus accumbens (NAcc) responses to negative feedback given by human partners compared to the computer partner. In contrast, NAcc reactivity to negative human feedback was enhanced compared to computer feedback in participants with low loneliness scores (LL). Shaded areas show the standard error of the mean of the fitted responses based on the hemodynamic response function. For illustration purpose, clusters are shown with significance levels of $P < 0.05$ uncorrected. Abbreviations: L, left, R, right.

Fig. 4. Functional connectivity during the social gambling task. Participants with high loneliness scores (HL) showed enhanced functional connectivity of the nucleus accumbens (blue sphere) with a cluster including the hippocampus while receiving negative human (vs. computer) feedback compared to participants with low loneliness scores (LL). Functional connectivity positively correlated with the pleasantness ratings of the negative human feedback (compared to the negative computer feedback). The dashed line represents the 95%-confidence interval of the plotted regression line. Bars represent group means. Error bars indicate standard errors of the mean. Abbreviations: L, left, R, right. * $P < 0.05$, *** $P < 0.001$.

Fig 5. Interactions of loneliness with social anxiety (SA). (**A**) Moderation analyses revealed that the positive association of SA with right amygdala activation during risky social decision-making (risky decision human – safe decision human) as observed in participants with low loneliness scores (LL; β = 0.63, *P* = 0.007, 95 % CI: [0.18, 1.08]) was not evident in participants with high loneliness scores (HL; β = -0.26, *P* = 0.17, 95 % CI: [-0.63, 0.11]). (**B**) Likewise, the positive relationship of SA with right amygdala activation during social decision-making contrasted with risky decisions involving a computer partner vanished in the HL group (LL: β = 0.69, *P* = 0.003, 95 % CI: [0.25, 1.14]; HL: β = 0.07, *P* = 0.72, 95 % CI: [-0.30, 0.43]). (**C**) Moreover, the non-significant negative association of SA with the subjective value of engaging in a social situation (i.e., CE50, the payoff offered in the safe option associated with 50% of safe decisions) in the LL group (β = -0.17, *P* = 0.48, 95 % CI: [-0.64, 0.30]) was reversed in the HL group (β = 0.40, *P* = 0.049, 95 % CI: [0.002, 0.80]). Thus, higher SA symptomatology was even associated with increased subjective values of engaging in social situations for participants suffering from loneliness. The dashed lines represent the 95%-confidence interval of the plotted regression lines.

Table 1. Whole-brain findings during decision-making across groups

Region	Right/left	Cluster size (voxel)	Peak *T*	MNI coordinates		
				x	y	z
Decision human > decision computer						
Medial orbitofrontal gyri	bil.	351	6.28	2	44	-14
Precuneus	bil.	800	6.04	4	-56	28
Risky decision > safe decision						
Inferior frontal gyrus, triangularis	R	2,218	8.77	44	24	24
Middle occipital gyrus	L	588	7.65	-44	-68	4
Fusiform gyrus	L	249	7.29	-22	-80	-8
Middle temporal gyrus	R	452	6.77	42	-58	10
Lingual gyrus	R	595	6.60	4	-80	-4
Anterior cingulate cortex	bil.	331	6.26	8	-14	30
Precentral gyrus	L	557	6.15	-42	-6	48
Supplementary motor area	R	633	6.09	8	8	60
Supramarginal gyrus	R	313	6.07	44	-40	14
Superior parietal gyrus	L	203	5.99	-26	-52	48
Superior temporal gyrus	R	110	5.90	50	-22	-4
Inferior temporal gyrus	L	120	5.73	-40	-44	-14
Superior occipital gyrus	L	220	5.58	-14	-66	38
Insular cortex	L	214	5.47	-30	26	2
Inferior parietal gyrus	R	139	5.28	28	-52	52

Risky decision human > risky decision computer

Superior temporal gyrus	R	448	7.60	48	-40	10
Precuneus	bil.	496	6.64	6	-56	28
Medial orbitofrontal gyri	bil.	328	5.79	2	42	-14
Inferior frontal gyrus, triangularis	R	315	5.49	42	16	22

Notes. Cluster-sizes are based on the initial cluster-forming height threshold of $P < 0.001$. Peak *T* and MNI coordinates are listed for FWE-corrected *P*s < 0.05 on peak level. No cluster survived the FWE-correction on the peak level for the safe decision human > safe decision computer contrast. Abbreviations: bil., bilateral; L, left; MNI, Montreal Neurological Institute; R, right.

Table 2. Whole-brain findings during the feedback phase across groups

Region	Right/left	Cluster size (voxel)	Peak *T*	MNI coordinates		
				x	y	z
Human feedback > computer feedback						
Middle temporal gyrus	R	6,837	12.07	54	-40	8
Calcarine fissure	R	141	12.01	22	-94	-2
Amygdala	L	3,273	9.66	-22	-8	-12
Fusiform gyrus	R	361	9.29	40	-48	-16
Fusiform gyrus	L	296	8.44	-38	-48	-20
Middle occipital gyrus	L	32	7.65	-20	-94	-2
Gyri rectus	bil.	295	6.54	6	38	-16
Inferior occipital gyrus	R	42	5.29	44	-76	-6
Positive feedback > negative feedback						
Inferior occipital gyrus	R	341	8.32	26	-92	-2
Caudate nuclei	bil.	2,792	8.10	8	10	-2
Middle cingulate gyri	bil.	2,897	6.80	-2	-34	34
Inferior occipital gyrus	L	101	6.63	-28	-88	-6
Angular gyrus	L	3,721	6.15	-40	-66	46
Middle frontal gyrus	L	2,771	6.11	-30	16	52
Precentral gyrus	R	2,059	5.62	36	-28	62
Superior frontal gyrus	R	722	5.59	20	34	48
Inferior orbitofrontal gyrus	L	55	5.53	-26	30	-16

Fusiform gyrus	L	229	5.43	-26	-46	-18
Positive human feedback > negative human feedback						
Caudate nuclei	bil.	685	7.52	8	10	-2
Angular gyrus	L	937	6.23	-40	-68	34
Middle temporal gyrus	R	1,487	6.09	56	-36	6
Middle temporal gyrus	L	551	5.63	-58	-42	10
Middle temporal gyrus	L	280	5.47	-48	-70	6
Precentral gyrus	R	1,087	5.31	40	-26	64

Notes. Cluster-sizes are based on the initial cluster-forming height threshold of $P < 0.001$. Peak *T* and MNI coordinates are listed for FWE-corrected *P*s < 0.05 on peak level. For the positive feedback > negative feedback contrast, the nucleus accumbens is included in the caudate nuclei cluster. Abbreviations: bil., bilateral; L, left; MNI, Montreal Neurological Institute; R, right.

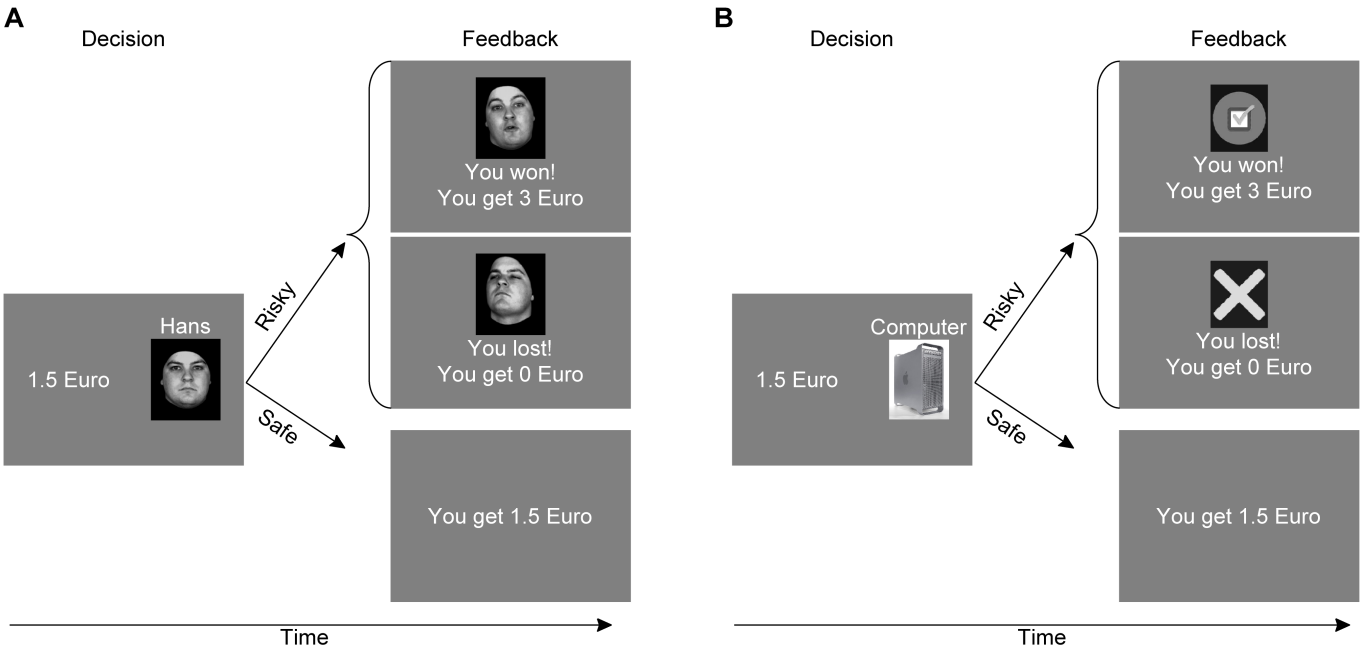

C

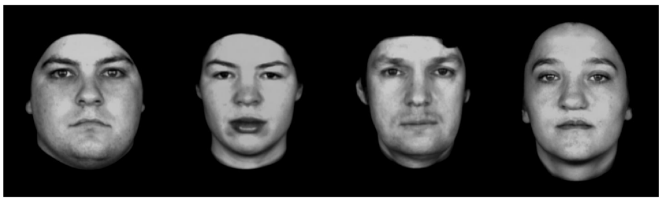

D

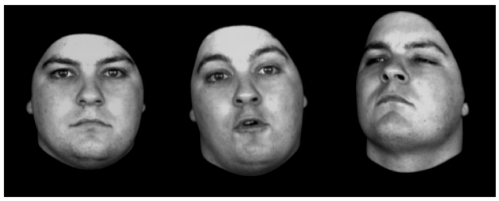

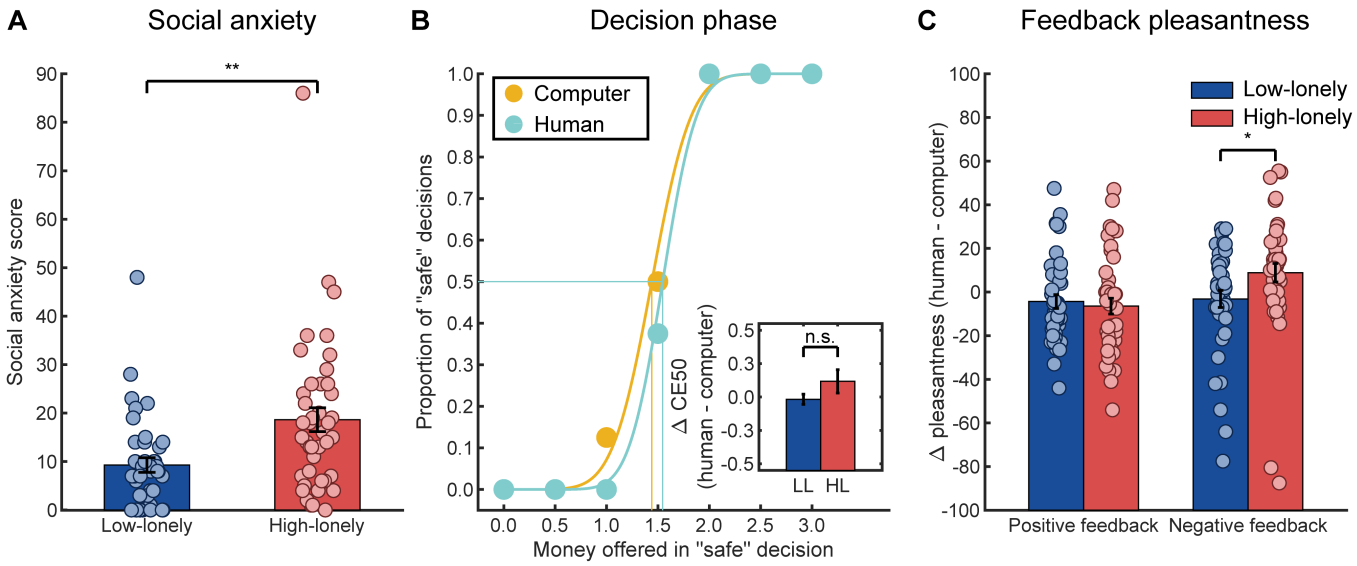

A

Amygdala

(risky decision human > risky decision computer)

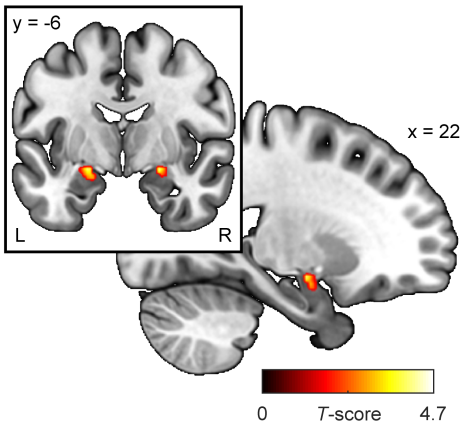

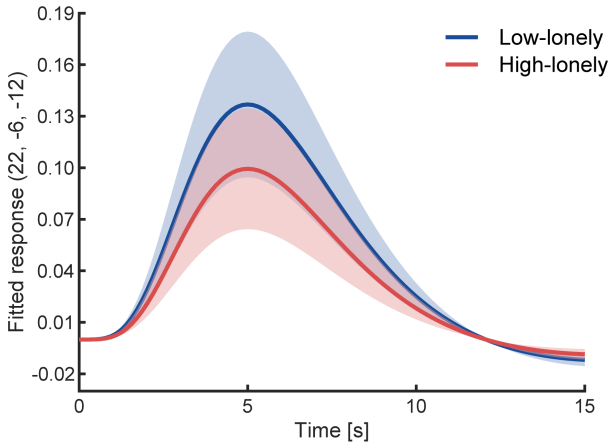

B

Nucleus accumbens

(LL (negative human feedback > negative computer feedback) > HL (negative human feedback > negative computer feedback))

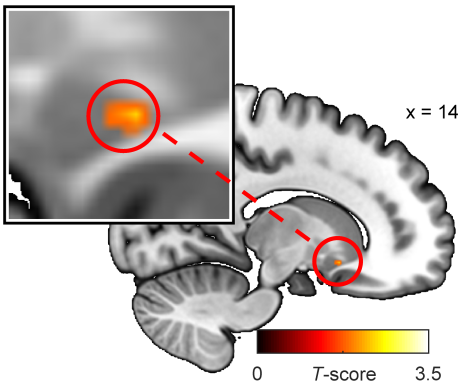

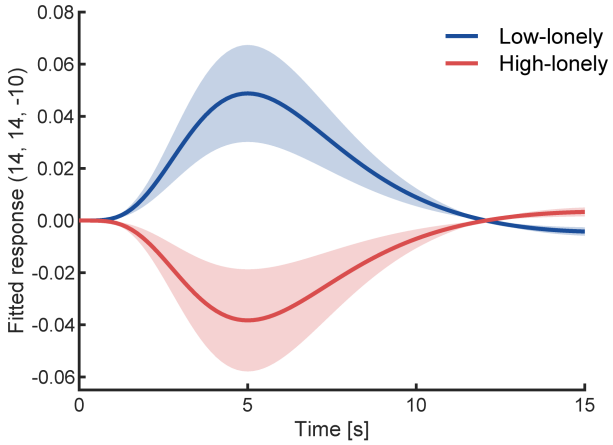

Left nucleus accumbens-hippocampal functional connectivity

(HL $_{\text{(negative human feedback > negative computer feedback)}}$ > LL $_{\text{(negative human feedback > negative computer feedback)}}$)